ARTICLE

High binding yet accelerated guest rotation within a cucurbit[7]uril complex. Toward paramagnetic gyroscopes and nanomachines.

G. Casano,[a] F. Poulhès,[a] T. K. Tran,[a] M. M. Ayhan,[a,b] H. Karoui,[a] D. Siri,[a] A. Gaudel-Siri,[a] A. Rockenbauer,[c] G. Jeschke,[d] D. Bardelang,[a*] P. Tordo[a*] and O. Ouari[a*]

The (15-oxo-3,7,11-triazadispiro[5.1.5.3]hexadec-7-yl) oxidanyl), a bis-spiropiperidinium nitroxide derived from TEMPONE can be included in cucurbit[7]uril to form a strong ($K_a \sim 2 . 10^5$ M^{-1}) CB[7]@**bPTO** complex. EPR and MS spectra, DFT calculations, and unparalleled increased resistance (~ factor 10^3) toward ascorbic acid reduction, show evidence for deep inclusion of **bPTO** inside CB[7]. The unusual shape of the CB[7]@**bPTO** EPR spectrum can be explained by an anisotropic Brownian rotational diffusion, the global tumbling of the complex being slower than rotation of **bPTO** around its "long molecular axis" inside CB[7]. The CB[7] (stator) with the encapsulated **bPTO** (rotator) behaves as a supramolecular paramagnetic rotor with increased rotational speed of the rotator that could be of interest for advanced nanoscale machines requiring wheels such as cucurbiturils with virtually no friction between wheel and axle for optimum wheel rotation (i. e. nanopulleys, nanocars).

Introduction

Molecular machines are increasingly being considered as promising architectures for advanced machineries proceeding at the nanoscale. Among the key components, cucurbiturils are symmetrical round-shape molecules[1-3] that can be used as molecular wheels for nanomachines such as small motor vehicle chassis. During the last two decades, the host-guest chemistry of CB[n] has been studied extensively[4,5] using a combination of electronic absorption and NMR spectroscopies, mass spectrometry, and X-ray crystallography. In the past few years, EPR spectroscopy has also been used as an additional tool to explore the binding properties of CB[n] with paramagnetic molecules, containing one or several nitroxide moieties as probes.[6-17] Lucarini first showed that TEMPO can be complexed by CB[7] ($K_a \sim 25 \pm 2 \times 10^3$ M^{-1}),[12] the free and complexed radical exchanging slowly on the EPR time scale, and the later showing smaller nitrogen hyperfine splitting and larger g factor values ($\Delta a_N = 0.11$ mT, $\Delta g = 0.0008$). Kaifer et al.[13] showed that the TEMPO moiety of 4-amido-2,2,6,6-tetramethylpiperidine-1-oxyl)cobaltocenium, is engulfed in CB[8] to form a very stable inclusion compound ($K_a = 2.1 \pm 1 \times 10^8$ M^{-1}). The binding of one and two CB[8] macrocycles has been used to allosterically regulate the extent of spin exchange coupling in paramagnetic molecules bearing several nitroxide moieties.[14] At concentrations above 10^{-3} M, an interesting selective aggregation of three supramolecules of nitroxide@CB[8] could be detected by EPR with various nitroxides.[15-17] The three supramolecules are arranged in a triangular geometry that leads to spin exchange between the three radical centers. No such aggregation was evident in the case of CB[7] complexes. Nitroxide probes are widely used to investigate biological systems,[6,18-21] however, their use in vivo is often limited by their rapid reduction to EPR silent compounds.[22-25] Various approaches have been developed to get nitroxide probes with increased resistance to bioreduction.[26-28] One strategy to protect nitroxides from bioreductants is to include them into macrocycles such as cyclodextrins (CD).[29-33] We[34-37] and others[38-41] have shown that the half-lives of various stable nitroxides or persistent nitroxide spin adducts[34] can indeed be enhanced in the presence of CDs. However, because of the relatively weak binding constants of CD@nitroxide complexes, reductants, such as glutathione (GSH) or ascorbate, still remain active. Recently, we reported that CB[7] is a promising candidate in protecting the TEMPO nitroxide in the presence of excess of ascorbate.[15] However, limitations still remain, due to the inherent dynamic inclusion complex equilibrium that leaves a fraction of the nitroxides exposed to the reductants. Recently different authors[42-44] reported that a high degree of size and shape complementarity, and the presence on the guest of two positive charges, both positioned to interact with the CB[7]'s ring carbonyl oxygens through ion-dipole interactions, can lead to unprecedented CB[7]-guest affinity, with values (up to $K_a = 7.2\times10^{17}$ M^{-1}) higher than that of the avidin-biotin pair. Based on these results, we designed nitroxides (2,2-dimethyl-4-oxo-1,9-diazaspiro[5.5]undec-1-yl)oxidanyl **PTO**, and **bPTO**, having in water one or two protonated amine functions prone to position near the two carbonyl laced portals, and to force the N-O• group to stand near the center of the CB[7] or CB[8] cavity (Scheme 1).
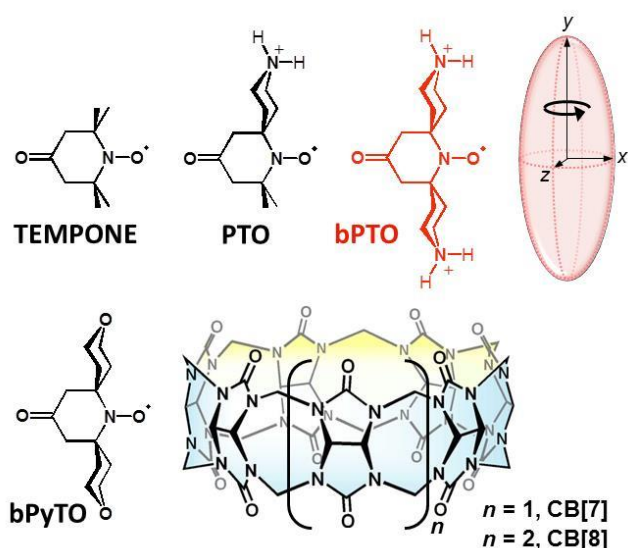
Scheme 1 Structures of TEMPONE derivatives and of cucurbit[*n*]urils.

Compared to **TEMPONE** we found that the binding affinities of **bPTO** for CB[7] and CB[8] are significantly increased, and once complexed **bPTO** becomes particularly resistant to reduction with ascorbate. Moreover, the EPR spectra of CB[7]@**bPTO** and CB[8]@**bPTO** complexes have a rather unusual shape. The high field line of the ^{14}N triplet is not broadened, as predicted due to the expected longer correlation time of the complexes compared to free **bPTO**. This behaviour can be explained by an anisotropic Brownian rotational diffusion, the global tumbling of the complexes being slower than the rotation of **bPTO** along its "long molecular axis" inside CB, the CB (stator) with the encapsulated **bPTO** (rotator) behaving as a supramolecular paramagnetic molecular rotor. Our results are presented and discussed hereafter.

Results and discussion

PTO and **bPTO** were prepared in a three-step sequence, experimental details for reaction procedures and characterizations are given in supplementary information (SI). All the experiments were performed in water, and with a pK_a of piperidine around 11.2, we will consider for the following discussion that **PTO** and **bPTO** are protonated at the amine sites.

Mass spectrometry. High resolution mass spectra of equimolar solutions of **bPTO** and CB[7] (1 mM) in water showed one peak at m/z 708.2644 corresponding to a doubly charged cation of formulae $C_{55}H_{66}N_{31}O_{16}^{2+}$ which agrees with the composition [(CB7)(**bPTO**•)]$^{2+}$. Similarly with CB[8], the detection of a cation at m/z 791.2893 corresponding to the formulae $C_{61}H_{72}N_{35}O_{18}^{2+}$ is in agreement with a complex of composition [(CB8)(**bPTO**•)]$^{2+}$.

EPR characterization. EPR spectra of **PTO** and **bPTO** show a typical three line pattern with a width at half height of 0.26 mT and 0.33 mT respectively and nitrogen coupling constants a_N of 1.57 and 1.53 mT respectively (g$_{PTO}$ = 2.0058, g$_{bPTO}$ = 2.0061, Figure 1). In regard with **TEMPONE** (0.08 mT),[45] the larger linewidth observed for **bPTO** is mainly due to additional long range hyperfine couplings with γ- and δ-hydrogens (see SI).
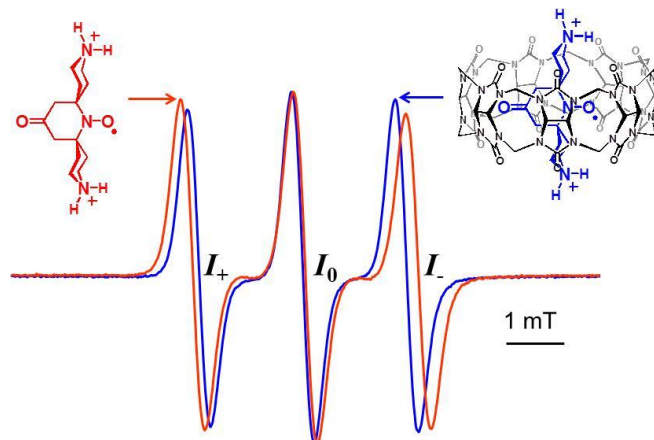

Fig. 1 EPR spectra in water of **bPTO** alone (0.2 mM, red line) and in the presence of CB[7] (1.4 eq., blue line), highlighting the reduced a_N coupling constant and the increased intensity of the high field line (I_-) upon binding.

Table 1. EPR parameters in water of nitroxides **PTO**, **bPTO**, their CB[*n*] complexes and relevant binding constants K_a.

	a_N / mT	K_a / M^{-1}
TEMPONE	1.61	-
TEMPONE/CB[7]	1.54	~10^3
TEMPONE/CB[8]	1.53	40
PTO	1.57	-
PTO/CB[7]	1.50	9.0×10^3
PTO/CB[8]	1.45	2.8×10^5
bPTO	1.53	-
bPTO/CB[7]	1.41	1.8×10^5
bPTO/CB[8]	1.40	$> 10^6$

For **bTPO**, in the presence of CB[7], the nitrogen hyperfine coupling constant decreases significantly (Δa_N = 0.12 mT) and the g factor increases (Δg = 0.0006), in agreement with the formation of a CB[7]@**bPTO** inclusion complex, which is accompanied by the N-O• group localization in the less polar surrounding of the CB[7] cavity. Usually, together with changes in a_N and g values, the formation of a nitroxide inclusion complex is accompanied by a broadening of the EPR high field line (I_-), resulting from an increase of the correlation time.[12,13] This broadening was not observed with CB[7]@**bPTO** (Figure 1), and as discussed below this result can be accounted for by an anisotropic rotational diffusion tensor for the included **bPTO**.

EPR titration experiments were performed recording a series of EPR spectra obtained by gradually increasing the CB[7] or CB[8] concentrations. Using a 2D simulation program,[46] binding constants K_a ~ 9×10^3 M^{-1} and 2.8×10^5 M^{-1} were determined (Table 1) for the complexation of **PTO** with CB[7] and CB[8] respectively. The significantly smaller K_a value obtained for CB[7] is presumably due to steric hindrance at the **PTO** carbonyl-nitroxide region (O-O• distance ≈ 7.7 Å with van der Waals radii with respect to the cavity of CB[7] (entrance ≈ 5.8 Å, inner part ≈ 7.8 Å). For **bPTO**, due to the presence of two piperidinium rings the affinity for CB[7] and CB[8] is expected to be higher. It reached 1.8×10^5 M^{-1} for CB[7] and was estimated (because we are close to the limit of reliable quantitative estimation of binding using EPR) to be

above 10^6 M^{-1} for CB[8]. The best fit between experimental and calculated EPR spectra was obtained assuming the formation of 1:1 complexes. Reduction experiments of the N-O$^\bullet$ group in the presence of ascorbic acid were performed (i) as an indication of the accessibility of the nitroxide function and (ii) as a way to determine the shielding effect, i. e. the efficacy of cucurbiturils to enhance the lifetime of nitroxides in biologically relevant media. Ascorbic acid was selected because it is known to be one of the most powerful reductants of nitroxides in biological fluids or cells, leading to the very fast decay of their EPR signals in biological systems.[23,47] We first monitored the EPR signals of included **bPTO** (0.1 mM) in CB[7] and CB[8] (0.35 mM) after addition of ascorbic acid (2 mM). Over 90 minutes, the signal decay was very slow while at the same ascorbic acid concentration, the nitroxide alone is instantaneously reduced (Figure 2).
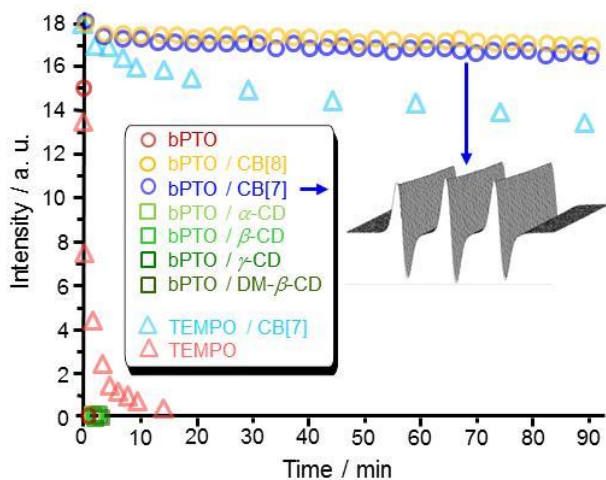

Fig. 2 Reduction experiments (decay of the EPR signal) of **bPTO** (0.2 mM ⭕) and TEMPO (0.1 mM △) and in the presence of CB[7] (12.75 mM for TEMPO (△) and 0.35 mM for **bPTO** ⭕), CB[8] (0.35 mM ⭕), α-CD (50 mM ☐), β-CD (10 mM ☐), γ-CD (100 mM ☐) and DM-β-CD (200 mM ☐) by ascorbic acid (2 mM, and sodium ascorbate: 2 mM for TEMPO and TEMPO / CB[7]).

Interestingly, α-cyclodextrin (α-CD 50 mM), β-cyclodextrin (β-CD 10 mM), γ-cyclodextrin (γ-CD 100 mM) and 2,6-di-*O*-methyl-β-cyclodextrin (DM-β-CD 200 mM) that also show signs of inclusion of **bPTO** (Fig 3a) afforded no protection, and no EPR signal could be detected 45 seconds after the addition of the reductant. These results show that CB[7] and CB[8] behave as effective shields around **bPTO**, and indicate that the N-O$^\bullet$ group is deeply immersed in their cavity. We previously showed that CB[7] (12.75 mM, 100-fold excess) improved the protection of TEMPO (0.1 mM) regarding ascorbate reduction (2 mM), increasing its half-life to 254 minutes.[15] The protection is much more efficient for **bPTO** (0.2 mM) with CB[7] (0.35 mM). The intensity of the CB[7]@**bPTO** EPR lines is reduced by only ~ 23% after 16 hours which corresponds to an approximate $t_{1/2}$ of ~ 17 h. Because in the same experimental conditions, the half-life time of **bPTO** alone is < 1 min, complexation with CB[7] affords an ca. 10^3 fold enhancement in the protection of the N-O$^\bullet$ group. Results obtained using CB[8] ($t_{1/2}$ ~ 21 h, SI) are very similar to those found with CB[7].

Rotational dynamics.

EPR studies. Inclusion of **bPTO** inside CB macrocycles is not accompanied by the usual broadening of the EPR high field line (I_-/I_0 = 0.897 and 0.964 for **bPTO** and CB[7]@**bPTO** respectively; I_+, I_0, and I_- are the peak-to-peak amplitudes of the low-field, central and high-field line respectively, Figure 1). To the best of our knowledge, it is the first time a slight increase of I_-/I_0 is observed after the formation of a CB@nitroxide inclusion complex. Different studies have shown that for a nitroxide the relative peak-to-peak amplitudes depend strongly on the rotational dynamics.[32,48-50] In order to get more details on this process, EPR spectra were fitted with the EasySpin[51] routine *chili* and home-written Matlab scripts. Results for CB[7]@**bPTO** are discussed hereafter, those concerning CB[8]@**bPTO** are given in SI. Two types of fits were performed. For the first type, the whole spectral lineshape was fitted with fixed ^{14}N hyperfine and *g* tensors principal values, and variable linewidth and rotational correlation time parameters. In the second type of fit, only the two ratios I_+/I_0 and I_-/I_0 were fitted (see SI). The first type of fit was performed with different models for the dynamics: isotropic Brownian rotational diffusion, anisotropic Brownian rotational diffusion with axial and orthogonal diffusion tensors, and assumption of an axial ordering potential. For axial tensors and the ordering potential, orientation of the unique axis along any of the molecular frame axes x (along the N-O bond), y, and z (along the p_π orbital lobes) was tested. We found that for an orthogonal rotational diffusion tensor the component along *z* was ill-defined. For all samples anisotropic Brownian rotational diffusion with an axial diffusion tensor and the unique axis along *y* and faster rotational diffusion about this unique axis gave the best fits (Table S1 and Figures S23). For **bPTO**, rotation about the *y* axis ($\tau_\parallel$ ~ 40-50 ps) was faster than rotation about the *x* and *z* axis ($\tau_\perp$ ~ 537 ps). For CB[7]@**bPTO,** rotation about the y axis increases ($\tau_\parallel$ ~ 13 ps), while rotation about the *x* and *z* axis is slightly slower ($\tau_\perp$ ~ 550 ps). Fits of the second type confirmed this trend. In the absence of CB, the ratios I_+/I_0 and I_-/I_0 could be perfectly fitted, providing rotational correlation times about the *y* axis between 30 and 40 ps for **bPTO**. Rotation about the *x* and *z* axes was slower by a factor ~16. For CB[7]@**bPTO**, the ratios could not be perfectly fitted although the trends observed experimentally were nicely reproduced. Rotational correlation time about the *y* axis apparently decreases to 0.4 ps, and the remaining deviation could be traced back to a relative intensity of the high-field line that is larger than can be achieved with this motional model or any model that we tested. The best approach to this high relative intensity is obtained if motion about the x and z axes is much slower (740 ps) than about the *y* axis.

Our results show that for CB[7]@**bPTO** the host and the guest have no dynamic cohesion. As previously mentioned by Mock,[52] the reason for an absence of mechanical coupling is the nearly cylindrical symmetry of cucurbiturils which allows guests to keep an axis of rotational freedom. However, usually the rotational motion of the complexed guest becomes restricted due to steric constraint.[42,52] For **bPTO**, slowdown of rotational diffusion about the *x* and *z* axes on inclusion into CB is expected because of the larger effective radius of the particle undergoing rotational diffusion. The fact that

rotational diffusion about the *y* axis remains fast and actually appears to speed up is unexpected. The data strongly suggest that **bPTO** rotates about its long axis after inclusion into **CB** with less friction than in pure water. This increase of rotational motion around the y axis could be reasonably accounted for by the successive formation of the same set of hydrogen bonds, between ammonium hydrogen atoms and the CB portal carbonyl groups, requiring a small energy barrier as in molecular ball bearing. In order to get more evidence on the rotational dynamics, we also examined the changes (Figure 3) in the EPR spectra of **bPTO** and **bPyTO**, in the presence of a large excess of 2,6-di-*O*-methyl-*β*-cyclodextrin (DM-*β*-CD) and CB[7] respectively.
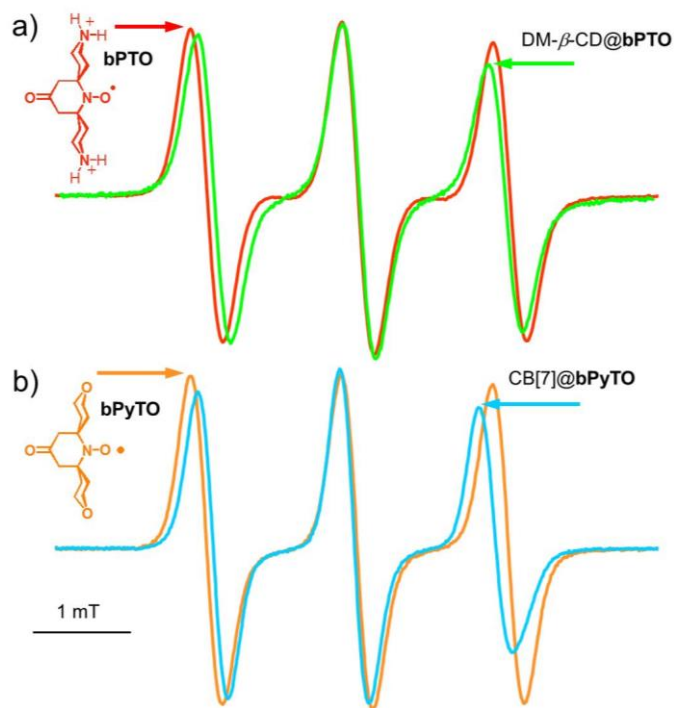

Fig. 3 EPR spectra of (a) **bPTO** (0.2 mM) alone (red line) and in the presence of DM-*β*-CD (200 mM, green line). (b) **bPyTO** (0.2 mM, orange line) and with CB[7] (8 mM, blue line).

In both cases, the observed decrease of a_N and the broadening of the high field line agree with the formation of an inclusion complex ($\Delta a_N = 0.07$ mT for DM-*β*-CD@**bPTO,** and $\Delta a_N = 0.1$ mT for CB[7]@**bPyTO**). Spectra calculations using the first type of fit indicated again the absence of dynamic cohesion. Interestingly, in the absence of either the CB[7] carbonyl groups for DM-*β*-CD@**bPTO** or the ammonium ions for CB[7]@**bPyTO** (Figure 3b), calculations predicted a slowing down (Table S1 and Figure S23) of the rotational dynamics after complexation.

We want to point out that the actual CB[7]@**bPTO** motion may be more complex, and the relative line intensities in the fast motion regime may not provide enough information for fully characterizing it. However, both type of EPR fits indicate a speed-up of rotational motion around the y axis, and we believe that the values from the

first type of fit are more realistic than the extreme speed-up found with the second type of fit.

DFT calculations. Although crystal structures of cucurbituril inclusion complexes are generally possible to obtain,[1-5,15,53-58] we were unsuccessful in getting crystals of CB[7]@**bPTO** and CB[8]@**bPTO**. DFT calculations were performed assuming that in these complexes, **bPTO** could adopt three main conformations (*trans-trans, trans-cis* and *cis-cis*) that differ in the geometry of the spiro junctions in regards with the N-O• bond (Scheme 2). For all the calculated conformers of the complexes, the two ammonium groups interact with the CB's ring carbonyl oxygens, resulting in a number of N-H•••O and C-H•••O stabilizing interactions.
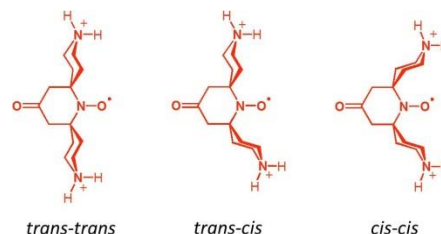
Scheme 2 Three favored conformers of **bPTO** which are very close in energy (within 0.3 kcal.mol⁻¹).
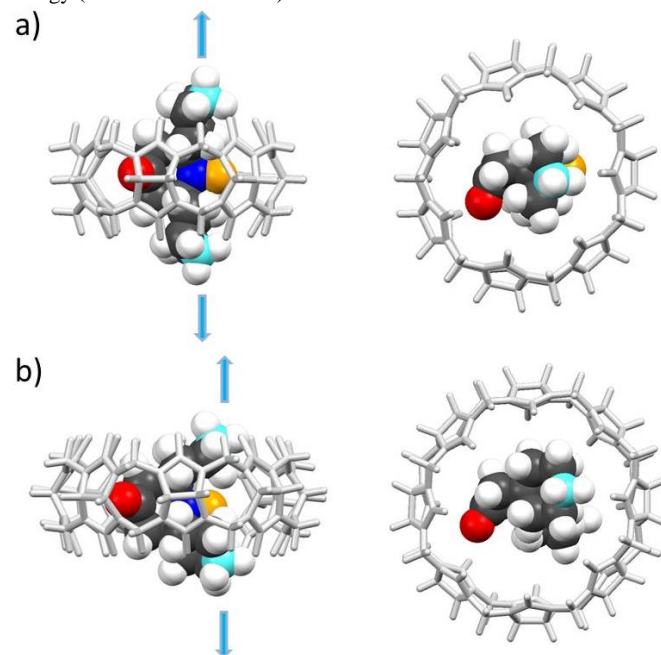

Fig. 4 Side and top views of the inclusion complex of **bPTO** in CB[7] (a, *trans-trans* conformer) and in CB[8] (b, *cis-cis* conformer) as found after DFT minimization (lowest energy structures) with water continuum (for other conformers, see SI; the colours of the N and O atoms of the N-O• group are dark blue and yellow respectively)

As shown in Figure 4, the N-O• group is strongly shielded, standing near the geometric center of the macrocycle. For CB[7]@**bPTO**, the distances between the CB[7] geometric center and the two ammonium nitrogens are 4.33 and 4.15 Å. The *trans-trans* conformer (Figure 4a) corresponds to the major conformer, the two others being at least 6 kcal.mol⁻¹ higher in energy (see SI). For this major conformer, the **bPTO** moiety is tightly bound, and the axis connecting the two nitrogen atoms of the piperidinium rings is colinear with the CB[7] C_7 axis. For
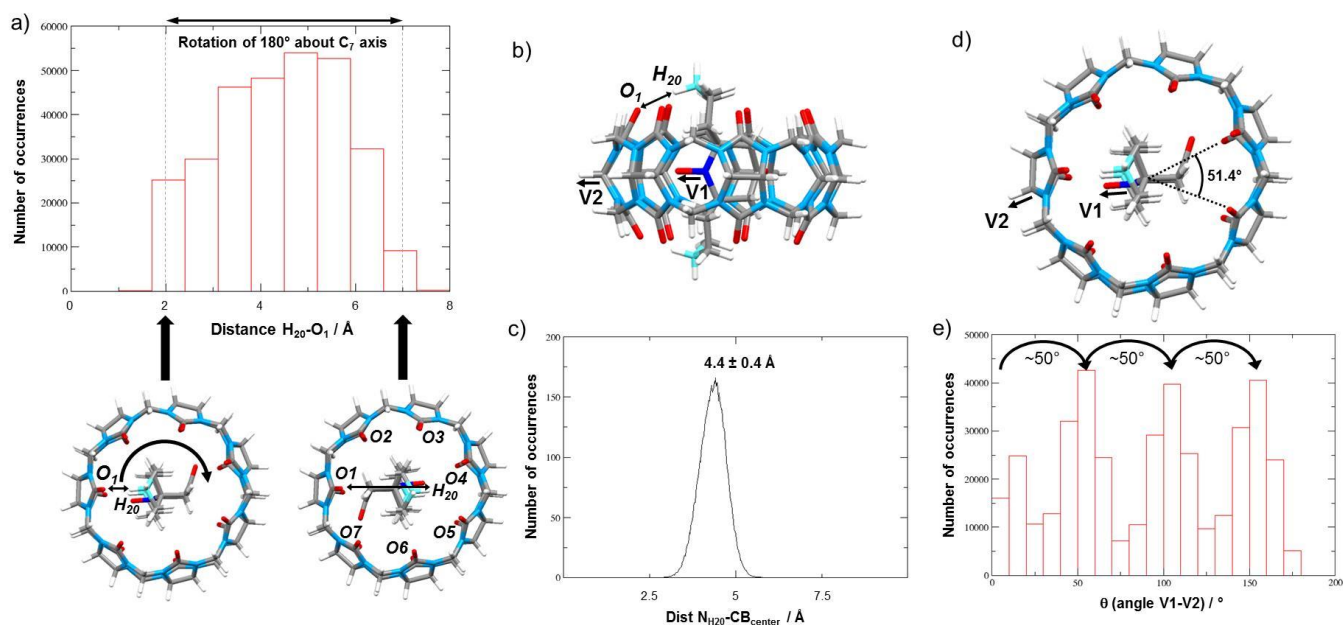
Fig. 5 a) Distribution of distances between guest atom H_{20} and host atom O_1 (b) for a 100 ns trajectory in water. c) Distance between the geometric center of CB[7] and the nitrogen atom carrying H_{20}. d) Vectors V1 and V2 defined as collinear with respect to the N-O• bond and a C-H bond of the cucurbituril. e) Distribution of θ values over two 100 ns trajectories, starting from θ = 0° and θ = 180° respectively.

CB[8]@**bPTO,** all three conformers have closer energies (within 2.3 kcal·mol^{-1}), reflecting higher degrees of freedom inside the larger macrocycle, and the axis connecting the two atoms of the piperidinium rings is tilted up to ≈ 24° from that of CB[8] C_8 axis (SI).

Molecular dynamics calculations. Molecular dynamics (MD) simulations in water, over 100 ns period, were performed for CB[7]@**bPTO** using Gromacs 5.0.4 package (see details in SI).[59] The results indicate that during the trajectory, the nitroxide guest stays deeply included in the cavity of CB[7] in agreement with EPR and DFT results. The distance between the CB[7] geometric center and the nitrogen atom carrying H_{20} (one ammonium hydrogen atom, Figure 5a) is nearly constant (4.4 ± 0.4 Å, Figure 5c), and the distance between H_{20} and the O_1 oxygen atom of CB[7], oscillates between 2 and 7 Å (Figure 5a). These results show that during a trajectory (i) the position of **bPTO** does not change significantly along the C_7 axis of the macrocycle (ii) **bPTO** rotates around the y-axis (Scheme 1) with the N-O• group remaining almost located in the plane passing through the CB[7] equatorial hydrogens. In agreement with this rotation, the angle θ between vectors V1 and V2 (respectively defined by the N-O and C-H bonds in Figure 5b) takes all the values between 0° and 180°. Figure 5e shows the distribution of θ values over two 100 ns trajectories, starting from θ = 0° and θ = 180° respectively. Interestingly, the value in between maxima is about 50°, an angle which corresponds to jumps of the ammonium hydrogen atoms from one carbonyl oxygen to another by steps ~ 2π/7 (Figure 5e).

There are few studies reporting guest rotational dynamics in molecular containers.[60-64] Because guests were reported to have slower dynamics when included in cucurbiturils,[42,52,65] the present acceleration of guest rotation upon binding was unexpected and represents an alternative solution to the oligoketone guest proposed by Keinan[66] for a "*lowered-friction*" molecular rotary motor. We think that the present jumping model where the hydrogen bonding ammonium function moves almost freely by increments of nearly 50°, is due to a preorganization of the CB[7] carbonyl crown where the ketone oxygen atoms are ready to hydrogen bond (on both sides of the CB) thus lowering the barrier to jump from one ketone to the next. In this view, the multiply hydrogen bonded network of bulk water (solvent shell) certainly plays a role because the two ammoniums of **bPTO** are less solvated when included in CB[7]. Such solvent *vs* preorganized macrocycle effect has already been reported for related systems[67,68] such as in lubricated molecular shuttles,[69] ring rotations within catenanes[70] or in simple N-arylimide molecules.[71] Still the present results may prove to be useful in the design of advanced CB[*n*] based molecular machines[72-75] like supramolecular gyroscopes[76-80] and molecular ball-bearing.[81] More generally, the present guest design offers new perspectives for any application requiring fast-spinning wheels were cucurbiturils can be used, as well as critical spinning information obtained from the free radical labelled guest and EPR spectroscopy.

Conclusion

Reduction of nitroxides is recognized to be one of the main limitations for their use in biology. We have shown that sequestration with high affinity in CB[7] or CB[8] of suitably-designed nitroxides, can dramatically improve their resistance to reduction (lifetime of several hours with minor decay in the presence of 20 fold excess of ascorbate). Our results could open new perspectives to the use of nitroxides in biological milieu. Additionally, our results highlight the advantages of cucurbiturils as stators offering restricted friction for optimized rotational motion in tailored molecular rotors. Such non covalent molecular rotors can open new avenues toward nanoscale molecular machines on which one could exert control over the rotator for fast spinning movements such as nanopulleys and all nanoscale machines where pulleys are

involved or for the construction of small motor vehicle chassis such as nanomotorcycles or nanocars.

Acknowledgements

Notes and references

[a] Aix-Marseille Université, CNRS, Institut de Chimie Radicalaire, UMR 7273, 13013 Marseille, France. Fax: 00 33 4 91 28 87 58; Tel: 00 33 4 91 28 86 10; E-mails: david.bardelang@univ-amu.fr; paul.tordo@univ-amu.fr; olivier.ouari@univ-amu.fr.

[b] Department of Chemistry, Gebze Technical University, P.K.:141, 41400 Gebze, Kocaeli, Turkey.

[c] Institute of Materials and Environmental Chemistry, Hungarian Academy of Sciences, 1519 Budapest, P.O. Box. 286, and Department of Physics, Budapest University of Technology and Economics 1111 Budapest, Hungary.

[d] ETH Zurich, Laboratory of Physical Chemistry, Vladimir-Prelog-Weg 2, CH-8093 Zurich, Switzerland.

Electronic Supplementary Information (ESI) available: experimental details, syntheses, DFT and experimental and calculated EPR spectra. See DOI: 10.1039/b000000x/

1. J. Lagona, P. Mukhopadhyay, S. Chakrabarti and L. Isaacs, *Angew. Chem., Int. Ed.*, 2005, **44**, 4844–4870.

2. J. W. Lee, S. Samal, N. Selvapalam, H.-J. Kim and K. Kim, *Acc. Chem. Res.*, 2003, **36**, 621–630.

3. O. A. Gerasko, D. G. Samsonenko and V. P. Fedin, *Russ. Chem. Rev.*, 2002, **71**, 741–760.

4. K. I. Assaf and W. M. Nau, *Chem. Soc. Rev.*, 2015, **44**, 394–418.

5. E. Masson, X. Ling, R. Joseph, L. Kyeremeh-Mensah and X. Lu, *RSC Adv.*, 2012, **2**, 1213–1247.

6. D. Bardelang, M. Hardy, O. Ouari and P. Tordo, "Spin Labels and Spin Probes", in *Handbook of Free Radical Chemistry and Biology*, John Wiley & sons, 2012, **4**, 1965–2015.

7. S. Yi, B. Captain and A. E. Kaifer, *Chem. Commun.*, 2011, **47**, 5500–5502.

8. M. Porel, S. Jockusch, M. F. Ottaviani, N. J. Turro and V. Ramamurthy, *Langmuir*, 2011, **27**, 10548–10555.

9. E. Mileo, C. Casati, P. Franchi, E. Mezzina and M. Lucarini, *Org. Biomol. Chem.*, 2011, **9**, 2920–2924.

10. M. Spulber, S. Schlick and F. A. Villamena, *J. Phys. Chem. A*, 2012, **116**, 8475−8483.

11. I. Kirilyuk, D. Polovyanenko, S. Semenov, I. Grigorev, O. Gerasko, V. Fedin and E. Bagryanskaya, *J. Phys. Chem. B*, 2010, **114**, 1719–1728.

12. E. Mezzina, F. Cruciani, G. F. Pedulli and M. Lucarini, *Chem.– Eur. J.*, 2007, **13**, 7223–7233.

13. S. Yi, B. Captain, M. F. Ottaviani and A. E. Kaifer, *Langmuir*, 2011, **27**, 5624–5632.

14. D. Bardelang, G. Casano, F. Poulhès, H. Karoui, J. Filippini, A. Rockenbauer, R. Rosas, V. Monnier, D. Siri, A. Gaudel-Siri, O. Ouari and P. Tordo, *J. Am. Chem. Soc.*, 2014, **136**, 17570–17577.

15. D. Bardelang, K. Banaszak, H. Karoui, A. Rockenbauer, M. Waite, K. Udachin, J. A. Ripmeester, C. I. Ratcliffe, O. Ouari and P. Tordo, *J. Am. Chem. Soc.*, 2009, **131**, 5402–5404.

16. E. Mileo, E. Mezzina, F. Grepioni, G. F. Pedulli and M. Lucarini, *Chem.– Eur. J.*, 2009, **15**, 7859–7862.

17. N. Jayaraj, M. Porel, M. F. Ottaviani, M. V. S. N. Maddipatla, A. Modelli, J. P. Da Silva, B. R. Bhogala, B. Captain, S. Jockusch, N. J. Turro and V. Ramamurthy, *Langmuir*, 2009, **25**, 13820–13832.

18. L. J. Berliner, "Spin Labeling: A Modern Perspective", in *Stable Radicals*, John Wiley & sons, 2010, 521–534.

19. V. V. Khramtsov and J. L. Zweier, "Functional *in vivo* EPR Spectroscopy and Imaging Using Nitroxide and Trityl Radicals", *ibid*, 537–563.

20. M. A. Sowers, J. R. McCombs, Y. Wang, J. T. Paletta, S. W. Morton, E. C. Dreaden, M. D. Boska, M. F. Ottaviani, P. T. Hammond, A. Rajca and J. A. Johnson, *Nat. Commun.*, 2014, **5**, 5460.

21. A. Rajca, Y. Wang, M. Boska, J. T. Paletta, A. Olankitwanit, M. A. Swanson, D. G. Mitchell, S. S. Eaton, G. R. Eaton and S. Rajca, *J. Am. Chem. Soc.,* 2012, **134**, 15724–15727.

22. Y. Wang, J. T. Paletta, K. Berg, E. Reinhart, S. Rajca and A. Rajca, *Org. Lett.*, 2014, **16**, 5298–5300.

23. A. A. Bobko, I. A. Kirilyuk, I. A. Grigorev, J. L. Zweier and V. V. Khramtsov, *Free Radical Biol. Med.*, 2007, **42**, 404–412.

24. K. J. Liu, M. W. Grinstaff, J. Jiang, K. S. Suslick, H. M. Swartz and W. Wang, *Biophys. J.*, 1994, **67**, 896–901.

25. Ya. Y. Woldman, S. V. Semenov, A. A. Bobko, I. A. Kirilyuk, J. F. Polienko, M. A. Voinov and E. G. Bagryanskaya and V. V. Khramtsov, *Analyst*, 2009, **134**, 904–910.

26. J. T. Paletta, M. Pink, B. Foley, S. Rajca and A. Rajca, *Org. Lett.*, 2012, **14**, 5322–5325.

27. I. A. Kirilyuk, Y. F. Polienko, O. A. Krumkacheva, R. K. Strizhakov, Y. V. Gatilov, I. A. Grigorev and E. G. Bagryanskaya, *J. Org. Chem.*, 2012, **77**, 8016–8027.

28. A. A. Bobko, A. Ivanov and V. V. Khramtsov, *Free Radical Res.*, 2013, **47**, 74–81.

29. P. Franchi, M. Lucarini, E. Mezzina and G. F. Pedulli, *J. Am. Chem. Soc.*, 2004, **126**, 4343–4354.

30. G. Ionita, A. Caragheorgheopol, H. Caldararu, L. Jones and V. Chechik, *Org. Biomol. Chem.*, 2009, **7**, 598–602.

31. G. Ionita, V. Meltzer, E. Pincu and V. Chechik, *Org. Biomol. Chem.*, 2007, **5**, 1910–1914.

32. J. Martinie, J. Michon and A. Rassat, *J. Am. Chem. Soc.*, 1975, **97**, 1818–1823.

33. Y. Kotake and E. G. Janzen, *J. Am. Chem. Soc.*, 1989, **111**, 5138–5140.

34. H. Karoui, A. Rockenbauer, S. Pietri and P. Tordo, *Chem. Commun.*, 2002, **24**, 3030–3031.

35. D. Bardelang, A. Rockenbauer, H. Karoui, J. P. Finet, I. Biskupska, K. Banaszak and P. Tordo, *Org. Biomol. Chem.*, 2006, **4**, 2874–2882.

36. D. Bardelang, L. Charles, J. P. Finet, L. Jicsinszky, H. Karoui, S. R. A. Marque, V. Monnier, A. Rockenbauer, R. Rosas and P. Tordo, *Chem.– Eur. J.*, 2007, **13**, 9344–9354.

37. M. Hardy, D. Bardelang, H. Karoui, A. Rockenbauer, J.-P. Finet, L. Jicsinszky, R. Rosas, O. Ouari and P. Tordo, *Chem.– Eur. J.*, 2009, **15**, 11114–11118.

38. P. Franchi, M. Fani, E. Mezzina and M. Lucarini, *Org. Lett.*, 2008, **10**, 1901–1904.

39. M. Okazaki and K. Kuwata, *J. Phys. Chem.*, 1985, **89**, 4437–4440.

40. C. Ebel, K. U. Ingold, J. Michon and A. Rassat, *New J. Chem.*, 1985, **9**, 479–485.

41. C. Ebel, K. U. Ingold, J. Michon and A. Rassat, *Tetrahedron Lett.*, 1985, **26**, 741–744.

42. M. V. Rekharsky, T. Mori, C. Yang, Y. H. Ko, N. Selvapalam, H. Kim, D. Sobransingh, A. E. Kaifer, S. Liu, L. Isaacs, W. Chen, S. Moghaddam, M. K. Gilson, K. Kim and Y. Inoue, *Proc. Natl. Acad. Sci. U. S. A.*, 2007, **104**, 20737–20742.

43. L. Cao, M. Sekutor, P. Y. Zavalij, K. Mlinaric-Majerski, R. Glaser and L. Isaacs, *Angew. Chem. Int. Ed.*, 2014, **53**, 988–993.

44. S. Moghaddam, C. Yang, M. Rekharsky, Y. H. Ko, K. Kim, Y. Inoue and M. K. Gilson, *J. Am. Chem. Soc.*, 2011, **133**, 3570–3581.

45. S. R. Burks, M. A. Makowsky, Z. A. Yaffe, C. Hoggle, P. Tsai, S. Muralidharan, M. K. Bowman, J. P.Y. Kao and G. M. Rosen, *J. Org. Chem.*, 2010, **75**, 4737–4741.

46. A. Rockenbauer, T. Szabo-Planka, S. Arkosi and L. Korecz, *J. Am. Chem. Soc.*, 2001, **123**, 7646–7654.

47. G. I. Roshchupkina, A. A. Bobko, A. Bratasz, V. A. Reznikov, P. Kuppusamy and V. V. Khramtsov, *Free Radical Biol. Med.*, 2008, **45**, 312–320.

48. D. Kivelson *J. Chem. Phys.* 1960, *33*, 1094–1106.

49. A. Kh. Vorobiev, V. S. Gurman and T. A. Klimenko, *Phys. Chem. Chem. Phys.*, 2000, **2**, 379–385.

50. M. G. Santangelo, M. Levantino, A. Cupane and G. Jeschke, *J. Phys. Chem. B,* 2008, *112*, 15546–15553.

51. S. Stoll and A. Schweiger, *J. Magn. Reson.*, 2006, **178**, 42–55.

52. W. L. Mock and N.-Y. Shih, *J. Am. Chem. Soc.*, 1989, **111**, 2697–2699.

53. J. Heo, S.-Y. Kim, D. Whang and K. Kim, *Angew. Chem. Int. Ed.*, 1999, **38**, 641–643.

54. S. Lim, H. Kim, N. Selvapalam, K.-J. Kim, S. J. Cho, G. Seo and K. Kim, *Angew. Chem. Int. Ed.*, 2008, **47**, 3352–3355.

55. L. M. Heitmann, A. B. Taylor, P. J. Hart and A. R. Urbach, *J. Am. Chem. Soc.*, 2006, **128**, 12574–12581.

56. P. Thuéry, *Cryst. Growth Des.*, 2008, **8**, 4132–4143.

57. D. Bardelang, K. A. Udachin, D. M. Leek, J. Margeson, G. Chan, C. I. Ratcliffe and J. A. Ripmeester, *Cryst. Growth Des.*, 2011, **11**, 5598–5614.

58. D. Bardelang, K. A. Udachin, R. Anedda, I. Moudrakovski, D. M. Leek, J. A. Ripmeester and C. I. Ratcliffe, *Chem. Commun.*, 2008, **40**, 4927–4929.

59. B. Hess, C. Kutzner, D. van der Spoel and E. Lindahl, *J. Chem. Theory Comput.*, 2008, **4**, 435−447.

60. A. Scarso, H. Onagi and J. Rebek Jr., *J. Am. Chem. Soc.*, 2004, **126**, 12728–12729.

61. P. D. Kirchhoff, J.-P. Dutasta, A. Collet and J. A. McCammon, *J. Am. Chem. Soc.*, 1999, **121**, 381–390.

62. J. S. Mugridge, G. Szigethy, R. G. Bergman and K. N. Raymond, *J. Am. Chem. Soc.*, 2010, **132**, 16256–16264.

63. R. Kulasekharan, N. Jayaraj, M. Porel, R. Choudhury, A. K. Sundaresan, A. Parthasarathy, M. F. Ottaviani, S. Jockusch, N. J. Turro and V. Ramamurthy, *Langmuir*, 2010, **26**, 6943–6953.

64. H. Kitagawa, Y. Kobori, M. Yamanaka, K. Yoza and K. Kobayashi, *Proc. Natl. Acad. Sci. U. S. A.*, 2009, **106**, 10444–10448.

65. D. Banik, J. Kuchlyan, A. Roy, N. Kundu and N. Sarkar, *J. Phys. Chem. B*, 2015, **119**, 2310–2322.

66. I. B. Shir, S. Sasmal, T. Mejuch, M. K. Sinha, M. Kapon and E. Keinan, *J. Org. Chem.*, 2008, **73**, 8772–8779.

67. Francesco G. Gatti, Salvador León, Jenny K. Y. Wong, Giovanni Bottari, Andrea Altieri, M. Angeles Farran Morales, Simon J. Teat, Céline Frochot, David A. Leigh, Albert M. Brouwer and Francesco Zerbetto, *Proc. Natl. Acad. Sci. U. S. A.*, 2003, **100**, 10–14.

68. G. S. Kottas, L. I. Clarke, D. Horinek and J. Michl, *Chem. Rev.*, 2005, **105**, 1281–1376.

69. M. R. Panman, B. H. Bakker, D. den Uyl, E. R. Kay, D. A. Leigh, W. J. Buma, A. M. Brouwer, J. A. J. Geenevasen and S. Woutersen, *Nat. Chem.*, 2013, **5**, 929–934.

70. D. A. Leigh, A. Murphy, J. P. Smart, M. S. Deleuze and F. Zerbetto, *J. Am. Chem. Soc.*, 1998, **120**, 6458–6467.

71. B. E. Dial, P. J. Pellechia, M. D. Smith and K. D. Shimizu, *J. Am. Chem. Soc.*, 2012, **134**, 3675–3678.

72. Y. H. Ko, I. Hwang, H. Kim, Y. Kim and K. Kim, *Chem. Asian J.*, 2015, **10**, 154–159.

73. W. S. Jeon, E. Kim, Y. H. Ko, I. Hwang, J. W. Lee, S.-Y. Kim, H.-J. Kim and K. Kim, *Angew. Chem. Int. Ed.*, 2004, **44**, 87–91.

74. S. Angelos, N. M. Khashab, Y.-W. Yang, A. Trabolsi, H. A. Khatib, J. F. Stoddart and J. I. Zink, *J. Am. Chem. Soc.*, 2009, **131**, 12912–12914.

75. W. R. Browne and B. L. Feringa, *Nature Nanotech.*, 2006, **1**, 25–35.

76. A. I. Day, R. J. Blanch, A. P. Arnold, S. Lorenzo, G. R. Lewis and I. Dance, *Angew. Chem., Int. Ed.*, 2002, **41**, 275–277.

77. R. Pievo, C. Casati, P. Franchi, E. Mezzina, M. Bennati and M. Lucarini. *ChemPhysChem*, 2012, **13**, 2659–2661.

78. E. Mezzina, M. Fani, F. Ferroni, P. Franchi, M. Menna and M. Lucarini, *J. Org. Chem.*, 2006, **71**, 3773–3777.

79. K. Skopek, M. C. Hershberger and J. A. Gladysz, *Coord. Chem. Rev.*, 2007, **251**, 1723–1733.

80. C. A. Schalley, *Angew. Chem. Int. Ed.*, 2002, **41**, 1513–1515.

81. R. J. Blanch, A. J. Sleeman, T. J. White, A. P. Arnold and A. I. Day, *Nano Lett.*, 2002, **2**, 147–149.